

# One-dimensional versus two-dimensional correlation effects in the oxyhalides TiOCl and TiOBr

M. Hoinkis,<sup>1,2</sup> M. Sing,<sup>1</sup> S. Glawion,<sup>1</sup> L. Pisani,<sup>3</sup> R. Valentí,<sup>4</sup> S. van Smaalen,<sup>5</sup> M. Klemm,<sup>2</sup>  
S. Horn,<sup>2</sup> and R. Claessen<sup>1,\*</sup>

<sup>1</sup>*Experimentelle Physik 4 and Röntgen Research Center for Complex Material Systems, Universität Würzburg,  
D-97074 Würzburg, Germany*

<sup>2</sup>*Experimentalphysik II, Universität Augsburg, D-86135 Augsburg, Germany*

<sup>3</sup>*Department of Chemistry, Imperial College London, South Kensington Campus, London SW7 2AZ, United Kingdom*

<sup>4</sup>*Institut für Theoretische Physik, Universität Frankfurt, D-60054 Frankfurt, Germany*

<sup>5</sup>*Laboratory of Crystallography, University of Bayreuth, D-95440 Bayreuth, Germany*

(Received 5 October 2006; revised manuscript received 23 February 2007; published 25 June 2007)

We have performed a comparative study of the electronic structures of the spin-Peierls systems TiOCl and TiOBr by means of photoemission spectroscopy and density-functional calculations. While the overall electronic structure of these isostructural compounds is qualitatively similar, the bromide appears to be less one-dimensional. We present a quantitative analysis of the experimental dispersions in terms of exchange constant  $J$  and hopping integral  $t$ , as well as a discussion of the qualitative spectral features. From that, we conclude that despite the one-dimensional physics triggering the ground state in both compounds, a proper description of the normal-state electronic structure has to take into account the anisotropic frustrated interchain interactions on the underlying triangular lattice.

DOI: 10.1103/PhysRevB.75.245124

PACS number(s): 71.20.-b, 71.27.+a, 71.30.+h, 79.60.-i

## I. INTRODUCTION

Based on magnetic measurements and local-density approximation (LDA)+ $U$  calculations, the layered Mott insulator TiOCl was recently proposed to be electronically and magnetically quasi-one-dimensional and an unusual spin-Peierls compound.<sup>1</sup> Indeed, a true spin-Peierls ground state was identified for TiOCl, as well as for the isostructural TiOBr by revealing the lattice dimerization in x-ray-diffraction measurements.<sup>2,3</sup> For a conventional spin-Peierls system, one would expect only one phase transition; however, TiOCl and TiOBr possess two successive phase transitions at temperatures  $T_{c_1}=67$  K,  $T_{c_2}=91$  K and  $T_{c_1}=28$  K,  $T_{c_2}=47$  K, respectively. In the intermediate phase, an incommensurate superstructure was found that develops below  $T_{c_2}$ .<sup>4,5</sup> In a first-order transition at  $T_{c_1}$ , this order locks in, resulting in the commensurate order of the spin-Peierls ground state.<sup>4-6</sup> Also in contradiction to a canonical spin-Peierls scenario, both compounds display marked fluctuation effects in an extended temperature regime above  $T_{c_2}$ . For TiOCl, this was seen in magnetic resonance,<sup>7,8</sup> Raman<sup>9</sup> and infrared spectroscopy,<sup>10</sup> and specific-heat measurements.<sup>11</sup> For TiOBr, the importance of fluctuations was inferred from the infrared optical properties.<sup>12</sup> The origin of these fluctuations is still unclear but fluctuating orbital degrees of freedom can be ruled out due to the high energy of the lowest crystal-field excitation in the  $t_{2g}$  manifold.<sup>6,13,14</sup> From photoemission spectroscopy on TiOCl in connection with electronic structure calculations, we argued in a previous study that electronic correlations and/or spin-Peierls fluctuations might play an important role in this system.<sup>13</sup> The detailed behavior of the quasi-one-dimensional dispersions, however, is still not understood.

In this study, we compare the electronic structures of TiOBr and TiOCl well above the transition temperatures  $T_{c_1}$  and  $T_{c_2}$ . We present angle-integrated and angle-resolved pho-

toemission spectroscopy (ARPES) data, as well as complementary density-functional calculations. While TiOBr is less one-dimensional than TiOCl, we conclude from a detailed analysis of the experimental dispersions, as well as a discussion of the qualitative spectral features that probably a Hubbard-like model including the anisotropic frustrated interchain interactions on the underlying triangular lattice is best suited to capture the relevant physics dominating the single-particle excitation spectra of these compounds.

## II. TECHNICAL DETAILS

Single crystals of TiOCl were prepared by chemical-vapor transport from  $\text{TiCl}_3$  and  $\text{TiO}_2$ .<sup>15</sup> TiOBr crystals were synthesized in a similar way from  $\text{TiO}_2$  with a 40% excess of Ti and  $\text{TiBr}_4$ .<sup>3,15</sup>

Photoemission spectroscopy (PES) was performed using HeI radiation (21.22 eV) and an Omicron EA 125 HR electron energy analyzer. Fresh surfaces were prepared by *in situ* crystal cleavage with adhesive tape. The resulting surfaces were clean and atomically long-range ordered as evidenced by x-ray induced photoemission and low-energy electron diffraction, respectively. Since both TiOCl and TiOBr are insulators, sample charging was reduced by measuring at elevated temperatures, i.e., at 325 K in the case of TiOCl and at 360 K in the case of TiOBr. For TiOCl, we found from systematic temperature variations that the charging is almost negligible at and above  $\approx 370$  K. In this situation, the maximum of the Ti  $3d$  peak (see below) is located 1.45 eV below the experimental chemical potential  $\mu_{\text{exp}}$ , which corresponds to the Fermi edge position of a silver foil. The TiOCl spectra were aligned accordingly. The energy position of the Ti  $3d$  peak in TiOBr depends on the temperature in a very similar way. It was aligned to the same value of 1.45 eV below  $\mu_{\text{exp}}$ . The energy resolution amounted to 60 meV for the TiOCl

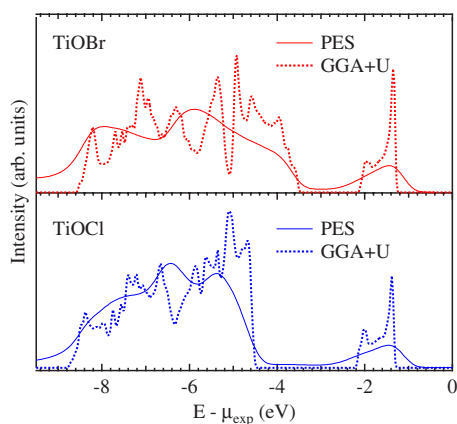


FIG. 1. (Color online) Angle-integrated photoemission spectra and GGA+ $U$  densities of states of TiOBr and TiOCl.

and 110 meV for the TiOBr measurements. The angular acceptance was  $\pm 1^\circ$  in both cases.

The photoemission experiments are complemented by calculations of the electronic structure of TiOBr and TiOCl within the *ab initio* density-functional theory in the generalized gradient approximation with inclusion of on-site Coulomb correlations (GGA+ $U$ ) (Refs. 16 and 17) using the full-potential linearized augmented plane-wave code WIEN2K.<sup>18</sup> The GGA+ $U$  calculations, which require a spin-polarized starting configuration, were performed by considering a ferromagnetic alignment of the Ti spins. For both systems, a value of  $RK_{\max}=7$  was used and 40 000 irreducible points were considered for Brillouin-zone integrations. The on-site Coulomb repulsion  $U$  and on-site exchange  $J_0$  were chosen to be 3.3 eV and 1 eV, respectively.<sup>1,19</sup>

### III. RESULTS AND DISCUSSION

In Fig. 1, angle-integrated photoemission spectra are compared to the GGA+ $U$  densities of states. The calculations yield a clear separation of the states with predominant Ti 3*d* character centered around  $-1.5$  eV from the ones which are mainly derived from the O and Br and/or Cl *p* levels. The latter are found between  $-8.5$  and  $-3.5$  eV for TiOBr and between  $-9$  and  $-4.5$  eV for TiOCl. The photoemission spectra clearly show this partition, as well. Also, the significantly smaller separation of the Ti 3*d* states from the rest of the valence band which is found in the calculations for TiOBr is observed in photoemission.

However, neither the exact shape nor the width of the Ti 3*d* spectral weight is reproduced by our calculations. As it was pointed out in an earlier publication,<sup>13</sup> this is most likely due to pronounced electronic correlations and/or spin-Peierls fluctuations which are beyond the scope of the GGA+ $U$  method. A better match between the calculated and the experimental spectra is found with respect to the width of the *p* bands. Due to matrix element effects, a more detailed agreement of the spectra with the bare densities of states cannot be expected.

In order to address the question of whether the smaller separation between the manifold of O and/or Cl(Br) and the

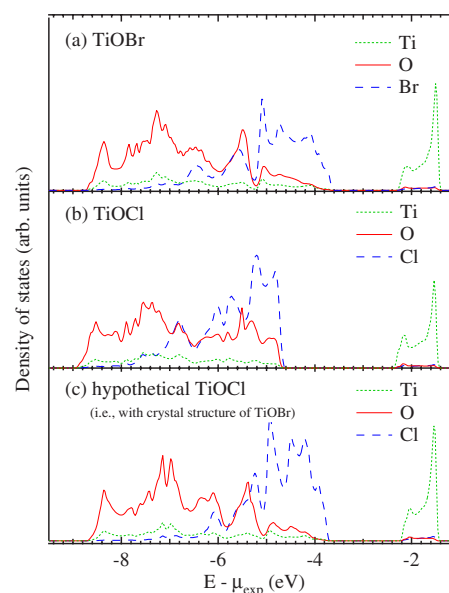


FIG. 2. (Color online) Atomically resolved GGA+ $U$  densities of states of (a) TiOBr, (b) TiOCl, and (c) a hypothetical compound with the crystal structure of TiOBr but with Br substituted by Cl.

Ti 3*d* states in the Br compared to the Cl system is caused by the change in chemistry or rather related to the structural expansion, we performed a third calculation. There, we assumed a hypothetical compound with the crystal structure of TiOBr but with Br substituted by Cl. In Fig. 2, the atomically resolved densities of states for all three systems are presented. The decomposition into Ti states near the chemical potential on the one hand and O and Cl(Br) states at higher binding energies on the other becomes very clear in this plot. By comparison, it is easily seen that the separation of the Ti states is smaller in the Br system mainly due to the expanded unit cell of TiOBr.

Turning to our angle-resolved photoemission data, we display energy distribution curves (EDCs) of both oxyhalides in Fig. 3. Panel (a) shows spectra of TiOBr along the crystallographic *b* direction in a broad energy range. What immediately stands out are the well-pronounced dispersions, especially in the Br 4*p* and/or O 2*p* part of the spectra. The dispersions are clearly symmetric with respect to the  $\Gamma$  point reflecting atomic long-range order and thus can be taken as a further proof of the good surface quality. Panels (b)–(e) focus on the Ti 3*d* spectral weight along the *a* and *b* axes. Following first the spectra along the *a* axis, i.e., from  $\Gamma$  to  $X$  in reciprocal space, both compounds exhibit a qualitatively similar behavior. Panels (b) and (c) show a single asymmetric peak throughout the Brillouin zone. Initially, its energy changes only slightly before it reaches a maximum and then shifts down in energy until the Brillouin-zone edge. Also, along the crystallographic *b* direction the EDCs for the two compounds qualitatively resemble each other [see panels (d) and (e)]. Starting from  $\Gamma$ , a single peak disperses upward, with the shape of the EDCs remaining essentially unaltered until  $\frac{1}{2}\Gamma Y$ . Subsequently, the overall dispersion bends downward reaching a minimum at the *Y* point which lies further below the one at  $\Gamma$ . At the same time, a new feature appears

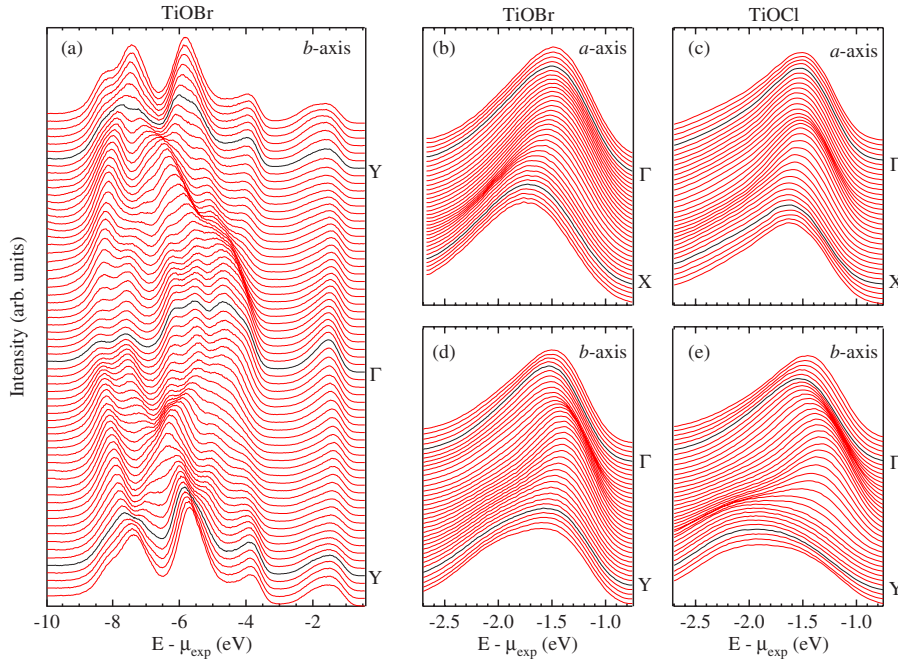


FIG. 3. (Color online) EDCs of TiOBr and TiOCl along the crystallographic  $a$  and  $b$  axes corresponding to the  $\Gamma X$  and  $\Gamma Y$  lines in the orthorhombic Brillouin zone, respectively. At the Ti  $3d$  energy, the X point corresponds to  $k=0.83 \text{ \AA}^{-1}$  for both compounds. The Y point corresponds to  $k=0.90 \text{ \AA}^{-1}$  for TiOBr and  $k=0.93 \text{ \AA}^{-1}$  for TiOCl.

at higher binding energies, so that the spectral shape is considerably broadened at the Y point.<sup>13</sup>

In Fig. 4, the same data sets are shown as intensity plots  $I(\mathbf{k}, E)$  in order to better compare the spectral weight dispersions of TiOBr and TiOCl. The four panels show the ARPES intensity along the crystallographic axes  $a$  and  $b$ , with the dispersions quantitatively identified by lines and markers. The lines indicate the EDC peak maxima obtained by a fitting procedure. For both compounds, this works well along the  $a$  direction and in the first half of the path from  $\Gamma$  to Y, i.e., along  $b$  in direct space. As already pointed out, in the

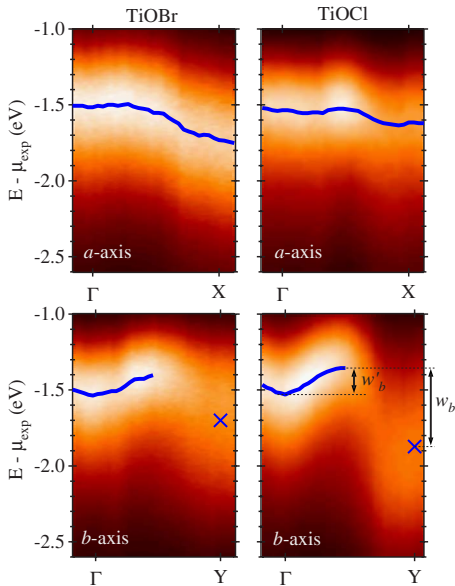


FIG. 4. (Color online) ARPES intensity plots  $I(\mathbf{k}, E)$  of TiOBr and TiOCl along the crystallographic axes  $a$  and  $b$ , corresponding to the  $X\Gamma X$  and  $Y\Gamma Y$  lines in the orthorhombic Brillouin zone. The lines indicate the peak positions of the EDCs. The crosses mark the first moment of the EDCs at the Y points.

second half the EDCs lose their single peaklike shape as an additional feature at higher binding energies appears, and thereby the spectra gradually change their form to a broad hump at the Y point. Thus, a fit with a single peak is not adequate here. Instead, we take the first-order moment of the EDCs at the Y point, indicated by crosses in Fig. 4. We emphasize once more that while at first glance the dispersions from the intensity plots might appear to be similar along the  $a$  and  $b$  directions, they are qualitatively different if one looks at the spectral shapes of the corresponding EDCs.

For a quantitative comparison of the electronic dispersions between the two compounds, we list the parameters  $w_a$ ,  $w_b$ , and  $w'_b$  in Table I. The unprimed quantities refer to the overall dispersion widths, while  $w'_b$  measures the width of only the inner part of the dispersion in the region from  $\Gamma$  to about  $\frac{1}{2}\Gamma Y$ . These widths are determined either from the difference of the maximal and minimal peak energies along the corresponding paths in  $k$  space as obtained by the fitting procedure (see lines in Fig. 4), or the difference between the maximum peak energy and the first-order moment at the Y point in the case of  $w_b$  (see markers in Fig. 4). The errors indicated reflect the scatter from several samples and measurements.

As is immediately read off from Table I, the overall dispersion width along  $b$  is significantly smaller in TiOBr with

TABLE I. Dispersions  $w_a$ ,  $w_b$ , and  $w'_b$  of the Ti  $3d$  weight in TiOBr and TiOCl, measured from the maximum to the minimum energy of the peak for the direction  $a$ , and from the maximum energy of the peak to the first moment of the Y point EDC for the direction  $b$ , respectively.

Width	TiOBr	TiOCl
$w_a$	0.27(3) eV	0.12(3) eV
$w_b$	0.26(5) eV	0.47(5) eV
$w'_b$	0.13(1) eV	0.17(1) eV

respect to TiOCl, while it is the other way round regarding the  $a$  axis. Given that both systems and, in particular, their electronic structures are governed by the same physics, we hence conclude that the anisotropy of TiOBr is less pronounced than in TiOCl. This is in line with the trend in the relevant hopping integrals as derived from downfolding LDA+ $U$  results, as well as with the fact that the Bonner-Fisher curve indicative for one-dimensional (1D) Heisenberg chains, does not provide a good fit for the high-temperature magnetic susceptibility of TiOBr in contrast to TiOCl.<sup>20,21</sup>

At this stage, we resort to the central result of our previous study on TiOCl,<sup>13</sup> where among various approaches to the  $k$ -resolved electronic structure we identified the spectral function of the single-band 1D Hubbard model as the most promising starting point in order to get further insight into the microscopic physics behind our experimental data. We recall that the most obvious discrepancies between the model calculations and experiment were the lack of any evidence for spin-charge separation and the absence of the so-called shadow band in the ARPES spectra although for the relevant parameter regime it should be clearly observable.<sup>22</sup> As possible explanations, we invoked multiorbital effects and/or spin-Peierls fluctuations. Beyond that, we note that temperature effects cannot account for this disagreement. While a drastic transfer of spectral weight masks the characteristic zero-temperature phenomenology in the metallic organic conductor tetrathia fulvalene-tetracyanoquinodi methane<sup>23,24</sup> (TTF-TCNQ) around room temperature (RT), temperature effects in the Mott insulator Na<sub>0.96</sub>V<sub>2</sub>O<sub>5</sub> (Ref. 25) at RT are weak enough to essentially preserve the zero-temperature spectral function. The reason is the characteristic energy scale,  $J$ ,<sup>26</sup> which roughly equals the thermal energy  $k_B T$  at RT in TTF-TCNQ but is about a factor of 2 larger in Na<sub>0.96</sub>V<sub>2</sub>O<sub>5</sub> and TiOCl.

A comparison between the isostructural compounds TiOBr and TiOCl now opens the possibility to further explore the reasons for this discrepancy between 1D Hubbard model prediction and experiment. For this purpose, we focus on the central part of the dispersion along the  $b$  axis marked by lines in Fig. 4. Within the single-band 1D Hubbard model, this part corresponds to the  $(\omega, k)$  region of the spinon and holon branches (see Fig. 7 in Ref. 13). Hence, depending on the dominant character of the experimental dispersion, its width  $w'_b$  should scale with either the exchange constant  $J$  whose value can be extracted from magnetic susceptibility measurements<sup>1,6</sup> or the hopping integral  $t$ . The latter either can be inferred from the Hubbard model perturbation expression for the exchange constant,  $J=4t^2/U$ , and thus should scale as  $t \propto \sqrt{J}$ , or can be deduced from an appropriate downfolding procedure of LDA+ $U$  band calculations.<sup>20</sup> An account of these quantities is given in Table II. The values of  $J$  for TiOBr and TiOCl differ by  $-45\%$  (with respect to the value in TiOCl), whereas the experimental dispersion width is smaller in TiOBr by only 23%.

On the contrary, the experimental width  $w'_b$  nicely matches the transfer integral as obtained from  $t=\sqrt{JU}/2$  which is smaller in the bromide by 26% compared to the chloride. A similarly fair agreement is achieved with  $t$  from the LDA+ $U$  downfolding studies<sup>20</sup> where the effective  $d_{xy}-d_{xy}$  hopping parameter along the  $b$  axis is by 19% smaller

TABLE II. Comparison of TiOBr and TiOCl with respect to various parameters possibly relevant for the observed dispersions: width of the central part of the Ti 3d spectral weight dispersion along  $b$  ( $w'_b$ ), exchange constant  $J$  obtained from the magnetic susceptibility (Ref. 6), hopping probability  $t$  derived from  $J$ , and the hopping integral  $t$  of downfolding LDA+ $U$  studies (Ref. 20).

	TiOBr	TiOCl	$\Delta x/x$
1D dispersion $w'_b$	0.13 eV	0.17 eV	$-23\%$
$J$ from magnetic susceptibility	32 meV	58 meV	$-45\%$
$t=\sqrt{JU}/2$	0.16 eV	0.22 eV	$-26\%$
$t$ from LDA+ $U$	0.17 eV	0.21 eV	$-19\%$

in TiOBr with respect to TiOCl. From this analysis, it follows that the experimentally observed dispersions scale with  $t$ —not with  $J$ —and thus can clearly be identified as charge excitations. Moreover, there is no indication in the spectra of Fig. 3 for any asymmetry toward lower binding energies which could be interpreted as a remnant of the spinon branch. Thus, we are led to rule out that the experimentally observed spectral dispersion is a superposition of both holon and spinon excitations.

Turning back to our starting point, i.e., the single-band 1D Hubbard model, a simple explanation for the lack of a spinon branch and shadow band would be that the two-dimensional coupling in these compounds under the particularities of a triangular lattice is already large enough so that generic 1D features of the spectral weight distribution cannot persist. One would then be left with a lower Hubbard band which, though incoherent in nature, could still display sizable dispersion alike to what we observe experimentally. Clearly, this issue demands for more detailed theoretical investigation. Alternatively, one could stick to the 1D Hubbard model and cite the coupling to phonons or multiorbital or spin-Peierls fluctuation effects as possible causes for the complete suppression of the generic 1D phenomenology. However, from the organic quasi-one-dimensional conductor TTF-TCNQ we know that the phonons,<sup>23,24</sup> which should couple equally strong to the electrons in this charge-density wave system and are of even higher energy, do not suppress or smear out the spectral features of spin-charge separation and shadow band. Moreover, since as already stated the orbital degrees of freedom are quenched in the oxyhalides and spin-Peierls fluctuations should not be too important so far above the transition temperatures, these two effects are probably not very effective.

In view of the above results, we are thus left in a situation where on the one hand the spin-Peierls ground state of both oxyhalides studied here is dominated by 1D interactions while the analysis and discussion of the electronic dispersions at room temperature, as well as the incommensurate order in the intermediate phase point to the importance of two-dimensional (2D) (frustrated) interchain interactions. It remains interesting to see whether or not an anisotropic Hubbard-model-type description taking account of the magnetic interchain frustrations on the underlying triangular lattice is capable of better describing the electronic properties of this class of materials positioned in the regime between 1D and 2D correlations.

## IV. CONCLUSIONS

In summary, we have investigated the electronic structure of TiOBr and TiOCl by means of photoelectron spectroscopy and GGA+ $U$  calculations. In these compounds, we find a very similar density of states, with the exception of an enlarged separation between the manifold of O and Cl(Br) levels and the Ti  $3d$  states. This difference is due to the enlarged unit cell in TiOBr. ARPES measurements reveal that the Ti  $3d$  spectral weight dispersions of the two compounds show a great qualitative resemblance, with the main difference that in TiOBr the overall dispersion width is larger along the  $a$  axis and smaller along the  $b$  axis, compared to the chloride. Thus, the quasi-one-dimensional character of TiOBr is clearly less pronounced. From the comparison of

TiOBr and TiOCl, we are able to show that the dispersion of the  $d$  band along the  $b$  axis scales with the square root of the exchange constant  $J$ , i.e., with the hopping integral  $t$ . Based on this analysis and the lack of any sign for spin-charge separation or shadow band and against the background of other experimental findings, we argue that the physics of both systems is governed by the interplay of both one-dimensional and two-dimensional correlations.

## ACKNOWLEDGMENTS

We are grateful to H. Benthien, F. Assaad, and M. Potthoff for fruitful discussions. This work was supported by the Deutsche Forschungsgemeinschaft through SFB 484 and Grant No. CL 124/3-3.

\*Electronic address: claessen@physik.uni-wuerzburg.de

- <sup>1</sup>A. Seidel, C. A. Marianetti, F. C. Chou, G. Ceder, and P. A. Lee, Phys. Rev. B **67**, 020405(R) (2003).
- <sup>2</sup>M. Shaz, S. van Smaalen, L. Palatinus, M. Hoinkis, M. Klemm, S. Horn, and R. Claessen, Phys. Rev. B **71**, 100405(R) (2005).
- <sup>3</sup>L. Palatinus, A. Schönleber, and S. van Smaalen, Acta Crystallogr., Sect. C: Cryst. Struct. Commun. **61**, i48 (2005).
- <sup>4</sup>S. van Smaalen, L. Palatinus, and A. Schönleber, Phys. Rev. B **72**, 020105(R) (2005).
- <sup>5</sup>A. Krimmel, J. Stempffer, B. Bohnenbuck, B. Keimer, M. Hoinkis, M. Klemm, S. Horn, A. Loidl, M. Sing, R. Claessen *et al.*, Phys. Rev. B **73**, 172413 (2006).
- <sup>6</sup>R. Rückamp, J. Baier, M. Kriener, M. W. Haverkort, T. Lorenz, G. S. Uhrig, L. Jongen, A. Möller, G. Meyer, and M. Grüninger, Phys. Rev. Lett. **95**, 097203 (2005).
- <sup>7</sup>T. Imai and F. C. Chou, arXiv:cond-mat/0301425 (unpublished).
- <sup>8</sup>V. Kataev, J. Baier, A. Möller, L. Jongen, G. Meyer, and A. Freimuth, Phys. Rev. B **68**, 140405(R) (2003).
- <sup>9</sup>P. Lemmens, K. Y. Choi, G. Caimi, L. Degiorgi, N. N. Kovaleva, A. Seidel, and F. C. Chou, Phys. Rev. B **70**, 134429 (2004).
- <sup>10</sup>G. Caimi, L. Degiorgi, N. N. Kovaleva, P. Lemmens, and F. C. Chou, Phys. Rev. B **69**, 125108 (2004).
- <sup>11</sup>J. Hemberger, M. Hoinkis, M. Klemm, M. Sing, R. Claessen, S. Horn, and A. Loidl, Phys. Rev. B **72**, 012420 (2005).
- <sup>12</sup>G. Caimi, L. Degiorgi, P. Lemmens, and F. C. Chou, J. Phys.: Condens. Matter **16**, 5583 (2004).
- <sup>13</sup>M. Hoinkis, M. Sing, J. Schäfer, M. Klemm, S. Horn, H. Benthien, E. Jeckelmann, T. Saha-Dasgupta, L. Pisani, R. Valentí *et al.*, Phys. Rev. B **72**, 125127 (2005).
- <sup>14</sup>D. V. Zakharov, J. Deisenhofer, H.-A. K. von Nidda, P. Lunkenheimer, J. Hemberger, M. Hoinkis, M. Klemm, M. Sing, R. Claessen, M. V. Eremin *et al.*, Phys. Rev. B **73**, 094452 (2006).
- <sup>15</sup>H. Schäfer, F. Wartenpfehl, and E. Weise, Z. Anorg. Allg. Chem. **295**, 268 (1958).
- <sup>16</sup>J. P. Perdew, K. Burke, and M. Ernzerhof, Phys. Rev. Lett. **77**, 3865 (1996).
- <sup>17</sup>V. I. Anisimov, I. V. Solovyev, M. A. Korotin, M. T. Czyzyk, and G. A. Sawatzky, Phys. Rev. B **48**, 16929 (1993).
- <sup>18</sup>P. Blaha, K. Schwarz, and J. Luitz, WIEN2K, Technische Universität Wien, Vienna, 2001, <http://www.wien2k.at>
- <sup>19</sup>T. Saha-Dasgupta, R. Valentí, H. Rosner, and C. Gros, Europhys. Lett. **67**, 63 (2004).
- <sup>20</sup>P. Lemmens, K. Y. Choi, R. Valentí, T. Saha-Dasgupta, E. Abel, Y. S. Lee, and F. C. Chou, New J. Phys. **7**, 74 (2005).
- <sup>21</sup>We remark that despite  $w_b/w_a \approx 1$  in TiOBr, it should not be considered as almost ideally two dimensional. Since the physical origin of the observed dispersions along  $a$  and  $b$  and hence their scaling properties are not known, their widths cannot be compared offhand.
- <sup>22</sup>H. Benthien, Ph.D. thesis, Universität Marburg, 2005.
- <sup>23</sup>R. Claessen, M. Sing, U. Schwingenschlögl, P. Blaha, M. Dressel, and C. S. Jacobsen, Phys. Rev. Lett. **88**, 096402 (2002).
- <sup>24</sup>M. Sing, U. Schwingenschlögl, R. Claessen, P. Blaha, J. M. P. Carmelo, L. M. Martelo, P. D. Sacramento, M. Dressel, and C. S. Jacobsen, Phys. Rev. B **68**, 125111 (2003).
- <sup>25</sup>K. Kobayashi, T. Mizokawa, A. Fujimori, M. Isobe, Y. Ueda, T. Tohyama, and S. Maekawa, Phys. Rev. Lett. **82**, 803 (1999).
- <sup>26</sup>A. Abendschein and F. F. Assaad, Phys. Rev. B **73**, 165119 (2006).